All-pass optical structures for repetition rate multiplication

Miguel A. Preciado and Miguel A. Muriel

ETSI Telecomunicacion, Universidad Politecnica de Madrid (UPM), 28040 Madrid, Spain.
ma.preciado@upm.es, muriel@tfo.upm.es

Abstract: We propose and analyze several simple all-pass spectrally-periodic optical structures, in terms of accuracy and robustness, for the implementation of repetition rate multipliers of periodic pulse train with uniform output train envelope, finding optimum solutions for multiplication factors of 3, 4, 6, and 12.

OCIS codes: (070.6760) Talbot and self-imaging effects; (140.4780) Optical resonators; (140.3538) Lasers, pulsed; (230.1150) All-optical devices; (320.7080) Ultrafast devices.

References and Links

1. K. Yiannopoulos, K. Vyrsokinos, E. Kehayas, N. Pleros, K. Vlachos, H. Avramopoulos, and G. Guekos, "Rate multiplication by double-passing Fabry-Perot filtering," IEEE Photon. Technol. Lett. **15**, 1294-1296 (2003).
2. D. S. Seo, D. E. Leaird, A. M. Weiner, S. Kamei, M. Ishii, A. Sugita, and K. Okamoto, "Continuous 500 GHz pulse train generation by repetition-rate multiplication using arrayed waveguide grating," Electron. Lett. **39**, 1138–1140 (2003).
3. P. Petropoulos, M. Ibsen, M. N. Zervas, and D. J. Richardson, "Generation of a 40-GHz pulse stream by pulse multiplication with a sampled fiber Bragg grating," Opt. Lett. **25**, 521–523 (2000).
4. B. Xia and L. R. Chen, "A direct temporal domain approach for pulse-repetition rate multiplication with arbitrary envelope shaping," IEEE J. Sel. Top. Quantum Electron. **11**, 165–172 (2005).
5. B. Xia and L. R. Chen, "Ring resonator arrays for pulse repetition rate multiplication and shaping," IEEE Photon. Technol. Lett. **18**, 1999-2001 (2006).
6. J. Caraquitena, Z. Jiang, D. E. Leaird, and A. M. Weiner, "Tunable pulse repetition-rate multiplication using phase-only line-by-line pulse shaping," Opt. Lett. **32**, 716-718 (2007).
7. Z. Jiang, C. -B. Huang, D. E. Leaird, and A. M. Weiner, "Spectral line-by-line pulse shaping for optical arbitrary pulse-train generation," J. Opt. Soc. Am. B **24**, 2124-2128 (2007).
8. C. -B. Huang and Y. Lai, "Loss-less pulse intensity repetition-rate multiplication using optical all-pass filtering," IEEE Photon. Technol. Lett. **12**, 167-169 (2000).
9. J. Azana and L. R. Chen, "Multiwavelength optical signal processing using multistage ring resonators," IEEE Photon. Technol. Lett. **14**, 654-656 (2002).
10. M. A. Preciado and M. A. Muriel, "Repetition rate multiplication using a single all-pass optical cavity," Opt. Lett. **33**, 962-964 (2008).
11. S. Arahira, S. Kutsuzawa, Y. Matsui, D. Kunimatsu, and Y. Ogawa, "Repetition-frequency multiplication of mode-locked pulses using fiber dispersion," J. Lightwave Technol. **16**, 405-410 (1998).
12. I. Shake, H. Takara, S. Kawanishi, and M. Saruwatari,"High-repetition-rate optical pulse generation by using chirped optical pulses," Electron. Lett. **34**, 792-793 (1998).
13. J. Azaña and M. A. Muriel, "Temporal Talbot effect in fiber gratings and its applications," Appl. Opt. **38**, 6700-6704 (1999).
14. S. Longhi, M. Marano, P. Laporta, and V. Pruneri, "Multiplication and reshaping of high-repetition-rate optical pulse trains using highly dispersive fiber Bragg gratings," IEEE Photon. Technol. Lett. **12**, 1498–1500 (2000).
15. J. Azaña, "Pulse repetition rate multiplication using phase-only filtering," Electron. Lett. **40**, 449-451 (2004).
16. A. V. Oppenheim, R. W. Schafer, and J. R. Buck, *Discrete-time signal processing* (Prentice-Hall ,1999).
17. S. Darmawan and M. K. Chin, "Critical coupling, oscillation, reflection, and transmission in optical waveguide-ring resonator systems," J. Opt. Soc. Am. B **23**, 834-841 (2006).
18. J. Capmany and M. A. Muriel, "A new transfer matrix formalism for the analysis of fiber ring resonators: compound coupled structures for FDMA demultiplexing," J. Lightwave Technol. **8**, 1904–1919, (1990).
19. J. Capmany, P. Muñoz, J. D. Domenech, and M. A. Muriel, "Apodized coupled resonator waveguides," Opt. Express **15**, 10196-10206 (2007).
20. G. Gavioli and P. Bayvel, "Amplitude jitter suppression using patterning-tolerant, all-optical 3R regenerator," Electron. Lett. **40**, 688-690 (2004).

#95428 - $15.00 USD Received 25 Apr 2008; revised 26 Jun 2008; accepted 1 Jul 2008; published 10 Jul 2008

1. Introduction

The generation of periodic pulse trains at repetition rates beyond those achievable by mode locking or direct modulation is very attractive for future ultrahigh-speed optical communication systems. One alternative is pulse repetition rate multiplication (PRRM) [1-15] of a lower rate source. In frequency domain, an ideal periodic pulse train is composed by a sequence of discrete spectral components, and PRRM techniques are based on periodically changing the amplitude and/or phase of these spectral components by linear filtering. This can be obtained by using a spectrally-periodic filter [1-10] as well as a non-spectrally-periodic filter (typically first order dispersive mediums) [11-14]. In particular, all-pass filtering PRRM methods [6-15] are highly desirable because of its intrinsic high energy efficiency.

In [10], a single all-pass optical cavity (APOC) for uniform envelope PRRM is analyzed in terms of accuracy and robustness, and it is found that, although theoretically three factors of repetition (2, 3 and 4) can be obtained for accurate uniform envelope PRRM, in practice robust solution can only be achieved for factor 2, resulting factor 3 solution specially tricky and unstable.

In this letter, we analyze several all-pass spectrally-periodic optical structures for 3×, 6×, 4× and 12× uniform envelope PRRM. It is worth noting that, although we focus on the ring resonator (RR) implementation of the APOCs, the results obtained can be easily extended to other APOC implementations. As it can be seen in Fig. 1, proposed optical structures are composed by 2-to-4 APOCs. It is demonstrated that, not only accurately uniform envelope but also robust solutions are found for proposed optical structures.

The remainder of this letter is as follows. In section 2, we explain some theoretical aspects about the design of the filter parameters in uniform envelope PRRM. In section 3, two different RR implementations (composed by two identical RR in cascade or coupled configuration) for 3× and 4× are proposed and analyzed, where the theory previously exposed is applied to design the RRs parameter. Moreover, we present optical structures for 6× and 12×, obtained by combining the 2×, 3×, and 4× implementations. In section 4, we analyze and discuss several practical examples of application. Finally, we summarize and conclude our work.

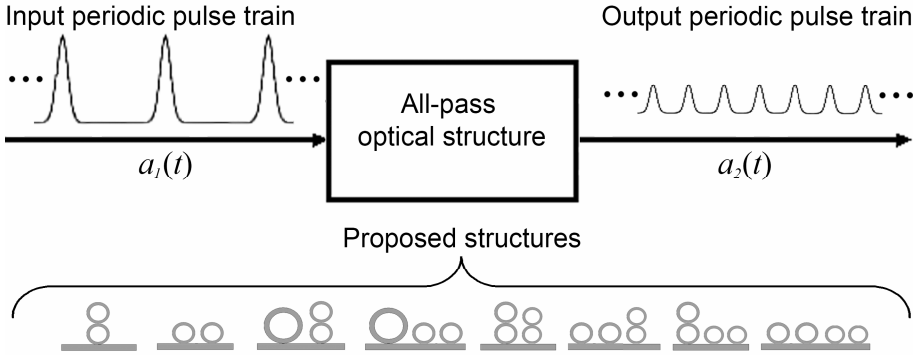

Fig. 1. Architecture of the system. The periodic pulse train is processed by the all-pass optical structure. Eight optical structures composed by multiple APOCs are proposed (RR implementation showed).

2. Filter parameters design for uniform Envelope PRRM

In the following, temporal signals are represented as complex envelopes with ω_0 as central carrier angular pulsation, and spectral signals are represented in the base-band angular pulsation $\omega=\omega_{opt}-\omega_0$, where ω_{opt} is the optical angular pulsation. Let us consider an input

#95428 - $15.00 USD Received 25 Apr 2008; revised 26 Jun 2008; accepted 1 Jul 2008; published 10 Jul 2008

periodic pulse train $a_1(t)=\sum_{n=-\infty}^{\infty} a_0(t-nT)$, where $a_0(t)$ represents the complex envelope of an individual pulse, and T is the temporal period of the signal. When a spectrally periodic filter $H(\omega)=H(\omega+2\pi FSR)$, is applied to the input pulse train $a_1(t)$, we obtain an output pulse train [10] $a_2(t)=\sum_{n=-\infty}^{\infty} C_n a_0(t-nT/N)$, with $\{C_n\}=\mathrm{IDFT}_n\{H(2\pi m/T)\}$, where FSR is the free spectral range, with $FSR \approx N/T$, N is the desired multiplication factor, IDFT_n denotes the n-th inverse discrete Fourier transform [16], {} denotes a sequence of N elements, C_n are complex coefficients, with $C_n=C_{n+N}$, and $m=1, 2,\ldots, N$. The magnitude of the sequence, $\{|C_n|\}$, describes the amplitude of the output pulse train envelope, which obviously is not affected by the phase of C_n. Since we are interested in uniform envelope PRRM with a multiplication factor N, we have to impose that all the terms of the sequence $\{|C_n|\}$ have the maximum uniformity. Thus, we can define a figure of merit (FM) for PRRM with uniform envelope as:

$$FM=\mathrm{var}\left(\{|C_n|\}\right)\Big/\mathrm{mean}\left(\{|C_n|\}\right) \tag{1}$$

where var($\{C_n\}$) and mean ($\{C_n\}$) denote the variance and mean of the sequence, respectively, and the function the optimum is $FM=0$. The variability of the solution can be estimated with the gradient magnitude $|\nabla FM|$. Both functions, FM and $|\nabla FM|$ must be taken into account in the optimization, indicating accuracy and robustness respectively.

3. APOC-based structures for 3×, 4×,6× and 12× PRRM

Structures based in a pair of identical RRs are proposed to obtain stable and exact solution for uniform envelope 3× and 4× PRRM. As it can be seen in Fig. 2, we propose two possible RRs configurations for each multiplication factor, in cascade and coupled.

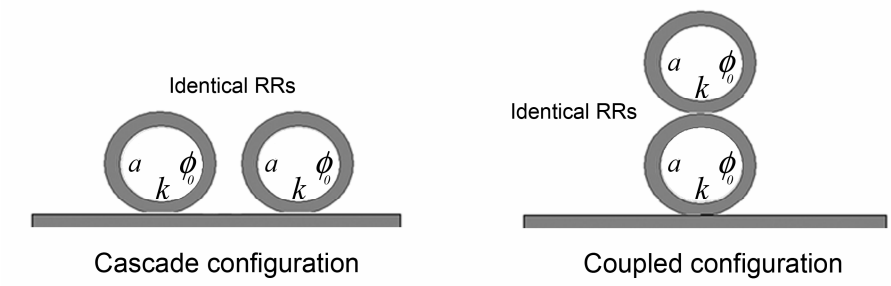

Fig. 2. All-pass optical structures for uniform envelope PRRM for 3× and 4× multiplication, both composed by two identical RR in cascade or coupled configuration.

The spectral response can be easily obtained for cascade configuration from:

$$H_{casc}(\omega)=\left(H_{single}(\omega)\right)^2=\left(\frac{r-a\cdot e^{-j\phi(\omega)}}{1-r\cdot a\cdot e^{-j\phi(\omega)}}\right)^2 \tag{2}$$

where $H_{single}(\omega)$ is the spectral response of a single RR [17], $r=(1-k)^{1/2}$ is the reflectivity of the RR coupler, k is the coupling factor, $a=\exp(-\alpha L_c/2)$ is the round-trip amplitude transmission factor, α is the power loss coeffient, L_c is the length of the round-trip length, and $\phi(\omega)$ is the round trip phase, with:

#95428 - $15.00 USD Received 25 Apr 2008; revised 26 Jun 2008; accepted 1 Jul 2008; published 10 Jul 2008

$$\phi(\omega) = \omega_{opt} / FSR = (\omega + \omega_0) / FSR = \omega / FSR + \phi_0 \tag{3}$$

where $\phi_0 = \omega_0 / FSR$ is the round-trip phase at $\omega_{opt} = \omega_0$. Since ω_0 is typically several orders higher than *FSR* and ϕ_0 can be arbitrarily added a multiple of 2π rad, we can easily deduce that a desired value of ϕ_0 can be adjusted by very small variations of *FSR*.

The coupled configuration structure spectral response can be obtained by the transfer model method [18,19]:

$$H_{coupled}(\omega) = \frac{r\left(1 - r \cdot a \cdot e^{-2j\phi(\omega)}\right) - \left(a \cdot e^{-j2\phi(\omega)}\right)\left(r - a \cdot e^{-j2\phi(\omega)}\right)}{\left(1 - r \cdot a \cdot e^{-j2\phi(\omega)}\right) - \left(r \cdot a \cdot e^{-j2\phi(\omega)}\right)\left(r - a \cdot e^{-j2\phi(\omega)}\right)} \tag{4}$$

These optical structures are characterized by the parameters of one of the RRs (since both RRs are identical). Supposing lossless RRs (a=1), these spectral responses, and therefore the figure of merit, can be parameterized with k and ϕ_0. Figure 3 shows $FM(k, \phi_0)$ and $|\nabla FM(k, \phi_0)|$ in a false-color representation for proposed 3× and 4× RR implementations (for coupled and cascade configurations in each case). Note that these functions present periodicity in the variable ϕ_0 with period $2\pi/N$, and have been limited for high values in order to increase the contrast of the plots. As it can be seen, robust and accurate solution, which correspond to dark blue in the false-color scale, can be simultaneously reached with the proposed configurations.

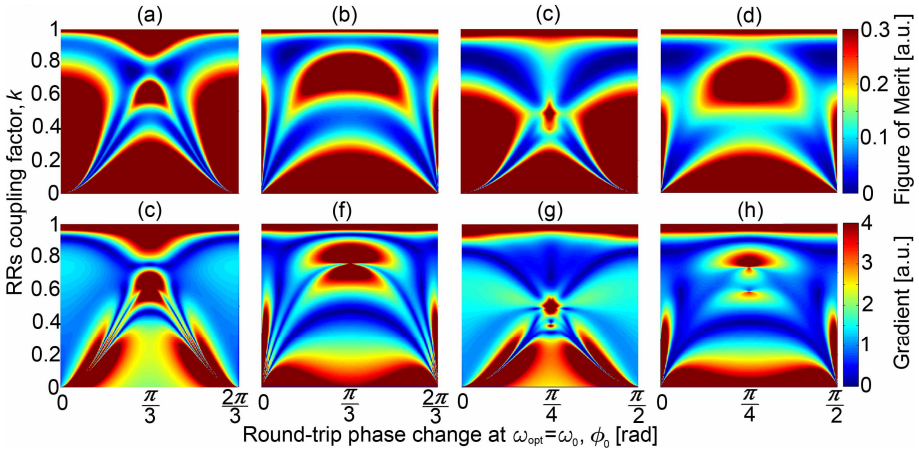

Fig. 3. Figure of merit and gradient function for [(a) and (e)] 3× coupled structure, [(b) and (f)] 3× cascade structure, [(c) and (g)] 4× coupled structure, and [(d) and (h)] 4× cascade structure.

Table 1 shows the optimum filter parameters set for 3× and 4× uniform envelope PRRM, where smoother region solutions have been selected in case of multiple optimum solutions, and 2× single RR optimum parameters obtained in [10] have been also included. It is worth noting that we have obtained the same optimum k parameter for 4× in both coupled and cascade configuration, and it is the same k value as obtained for 2× in [10]. Table 1 also includes the case of RR with losses, for a=0.95 and a=0.9. Proceeding similarly as above, we have calculated the optimum structures parameters. Moreover, RR losses affect to the energetic efficiency and uniformity of the pulse train envelope parameters. The energetic

#95428 - $15.00 USD Received 25 Apr 2008; revised 26 Jun 2008; accepted 1 Jul 2008; published 10 Jul 2008

efficiency can be calculated from $Eff[\%] = 100 \times \sum_{n=1}^{N} |C_n|^2$, and the PRRM envelope error is estimated with an error coefficient:

$$Err[\mathrm{dB}] = 20\log_{10}\left[\max\left(\{|C_n|\}\right) / \min\left(\{|C_n|\}\right) \right] \quad (5)$$

which indicates the maximum intensity peak variation in decibels (similar to peak-to-peak amplitude jitter [20]). The severity of *Err* and *Eff* values depends on the concrete application.

Table 1. Summary of the Optical Structures Parameters Values Corresponding to 2×, 3×, and 4× Uniform Envelope PRRM, for a = 1, a=0.95, and a=0.9.

N	Structure Configuration	a	k	ϕ_0 [rad]	*Err* [dB]	*Eff* [%]
2	Single	1	0.8284	1.571	0	100
		0.95	0.8287	1.571	0	92.45
		0.9	0.8298	1.571	0	55.55
3	Coupled	1	0.7393	0.8435	0	100
		0.95	0.7409	0.8207	0	74.45
		0.9	0.7450	0.8091	0	57.87
3	Cascade	1	0.8571	0.3335	0	100
		0.95	0.8579	0.3004	0	81.15
		0.9	0.8603	0.2552	0	66.17
4	Coupled	1	0.8284	0	0	100
		0.95	0.8120	0.2162	0.67	83.64
		0.9	0.8092	0.2691	1.51	69.65
4	Cascade	1	0.8284	0	0	100
		0.95	0.8316	0	1.65	81.45
		0.9	0.8390	0	3.11	67.06

Moreover, we can combine these filters to obtain higher multiplication factors. When combining spectrally periodic filters, the spectral responses of the resulting filter is the product of the spectral responses of the composing filters, and the *FSR* of the whole filter is equal to the minimum common multiple of the *FSR* of the filters. We have exact and stable RR based filters for 2×, 3×, and 4× PRRM, which *FSR* are respectively 2/*T*, 3/*T*, and 4/*T*. Thus, in order to get a higher *FSR* we have two possible combinations, 2× with 3×, obtaining *FSR*≈6/*T*, and 3× with 4×, obtaining *FSR*≈12/*T*. Since the resulting filters terms {|C_n|} preserve uniformity, 6× and 12× uniform envelope PRRM is performed. All the possible 6× and 12× optical structures obtained by combination of the previous 2×, 3× and 4× filters are showed in Fig. 4 (a) and (b), respectively.

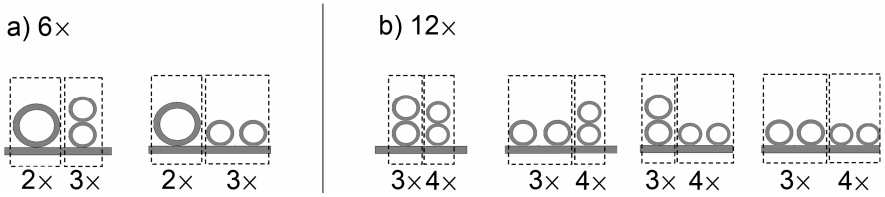

Fig. 4. All-pass optical structures for uniform envelope PRRM for (a) 6× multiplication and (b) 12× multiplication. These optical structures are composed by substructures corresponding to 2×, 3×, and 4× multiplication, which are marked with a dashed box.

#95428 - $15.00 USD Received 25 Apr 2008; revised 26 Jun 2008; accepted 1 Jul 2008; published 10 Jul 2008

4. Examples

In these examples we assume an input periodic pulse train with central frequency ($\omega_0/2\pi$)=192 THz, temporal period of T=100 ps (pulse repetition rate of 10 GHz), and lossless RRs (a=1). The FSR value for 2×, and 3× examples is a slightly different value to N/T in order to obtain the proper ϕ_0 value. Cascade-RRs configuration is chosen for 3×, which parameters are obtained from Table 1, with k_1=0.739 and FSR_1=30+2.488×10^{-4} GHz. For 4× we choose coupled-RRs configuration, with k_2=0.8284 and FSR_2= 40 GHz. We reuse these RRs implementations for 6× and 12×. Thus, combining the 3× designed filter with a 2× single-RR configuration, which optimum filter parameters are [10] k_3=0.8284 and FSR_3=20+5.208×10^{-4} GHz, we obtain the 6× optical structure. Finally, combining the 3× with the 4× designed filters, we obtain the 12× optical structure. Figure 5 shows the output pulse train intensity numerically obtained for these examples. Figure 6 shows the influence on the envelope error of frequency variations because of laser noise and ring fabrication errors for the previous examples, estimated with the envelope error coefficient used above, *Err*. Because of the temporal discrete RR response, these variations only affect to the output pulse train envelope, but not to the waveform of each individual pulse. It is worth noting the high robustness of the 4× filter, and the error accumulation in the 6× and 12× examples, which is clearly dominated by the error contribution of the 3× filter combined in both cases.

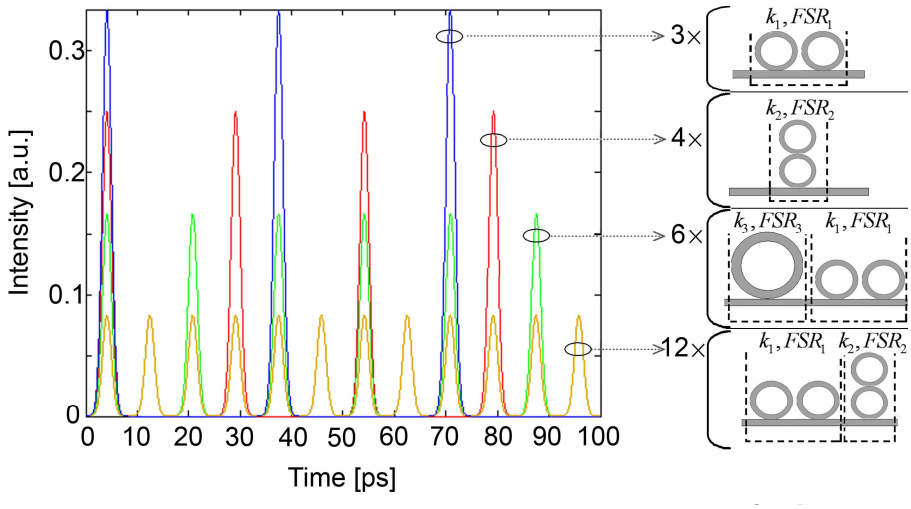

Fig. 5. Output-pulse-train intensity for 3×(blue), 4× (red), 6× (green), and 12× (yellow) uniform envelope PRRM corresponding to the examples, and the corresponding optical structures.

#95428 - $15.00 USD Received 25 Apr 2008; revised 26 Jun 2008; accepted 1 Jul 2008; published 10 Jul 2008

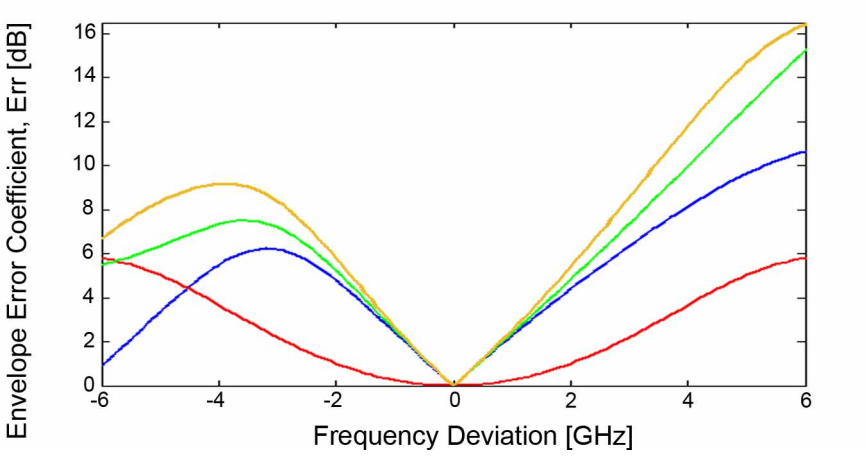

Fig. 6. Envelope error coefficient, *Err*, for 3×(blue), 4× (red), 6× (green), and 12× (yellow).

For RRs with losses, we have to set another RRs parameters, as it was showed in Table 1. It can be easily deduced that the $\{|C_n|\}$ sequence of the resulting filter can be obtained as the circular convolution of the $\{|C_n|\}$ sequences of the combining sub-filters, and from this, that *Err* and *Eff* of the resulting filter can be calculated respectively as the sum and product of the corresponding *Err* and *Eff* terms of the combining sub-filters. Thus, using Table 1, we can observe that 2×, 3×, and 6× configurations preserve perfect pulse train uniformity in a moderate losses range [$a \in (0.9, 1)$], but 4× and 12× examples do not preserve perfect uniformity (see *Err* in Table 1). However, energetic efficiency is affected by RR losses in all the cases (see *Eff* in Table 1).

5. Conclusion

In this letter we have proposed and analyzed several all-pass optical structures composed by 2-to-4 APOCs, which achieve robust and accurate uniform envelope PRRM with high energetic efficiency (ideally 100% for lossless RRs). For 3× and 4× PRRM, we have two different configurations, both composed by two identical RRs in cascade or coupled configuration. In the parameters design of these four filters (3× and 4× with coupled and cascade configuration), we have obtained accurate and robust solution without trade-off requirement (in contrast to [10]). For 6× and 12× PRRM, we have several optical structures obtained by combining filters of 2×, 3×, and 4× PRRM. We have also analysed the effect of RR losses on the energetic efficiency and the output pulse train envelope uniformity. In the examples, we have obtained readily feasible RR parameters, and we have observed the effect of combining filters in 6× and 12×.

Acknowledgments

This work was supported by the Spanish *Ministerio de Educación y Ciencia* under Project "Plan Nacional de I+D+I TEC2007-68065-C03-02".

#95428 - $15.00 USD Received 25 Apr 2008; revised 26 Jun 2008; accepted 1 Jul 2008; published 10 Jul 2008